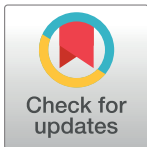# PLOS ONE

RESEARCH ARTICLE

Application of low-intensity pulsed therapeutic ultrasound on mesenchymal precursors does not affect their cell properties

Beatriz de Lucas[1], Laura M. Pérez[1], Aurora Bernal[2], Beatriz G. Gálvez[1]*

1 Faculty of Biomedical and Health Sciences, Universidad Europea de Madrid, Madrid, Spain, 2 Centro Nacional de Investigaciones Cardiovasculares (CNIC), Madrid, Spain

* beatriz.ggalvez@ufv.es

Abstract

Ultrasound is considered a safe and non-invasive tool in regenerative medicine and has been used in the clinic for more than twenty years for applications in bone healing after the approval of the *Exogen* device, also known as low-intensity pulsed ultrasound (LIPUS). Beyond its effects on bone health, LIPUS has also been investigated for wound healing of soft tissues, with positive results for various cell processes including cell proliferation, migration and angiogenesis. As LIPUS has the potential to treat chronic skin wounds, we sought to evaluate the effects produced by a conventional therapeutic ultrasound device at low intensities (also considered LIPUS) on the migration capacity of mouse and human skin mesenchymal precursors (s-MPs). Cells were stimulated for 3 days (20 minutes per day) using a traditional ultrasound device with the following parameters: 100 mW/cm² with 20% duty cycle and frequency of 3 MHz. At the parameters used, ultrasound failed to affect s-MP proliferation, with no evident changes in morphology or cell groupings, and no changes at the cytoskeletal level. Further, the migration and invasion ability of s-MPs were unaffected by the ultrasound protocol, and no major changes were detected in the gene/protein expression of ROCK1, integrin β1, laminin β1, type I collagen and transforming growth factor β1. Finally, RNA-seq analysis revealed that only 10 genes were differentially expressed after ultrasound stimulation. Among them, 5 encode for small nuclear RNAs and 2 encode for proteins belonging to the nuclear pore complex. Considering the results overall, while the viability of s-MPs was not affected by ultrasound stimulation and no changes were detected in proliferation/migration, RNA-seq analysis would suggest that s-MPs do respond to ultrasound. The use of 100 mW/cm² intensity or conventional therapeutic ultrasound devices might not be optimal for the stimulation the properties of cell populations. Future studies should investigate the potential application of ultrasound using variations of the tested parameters.

Introduction

Cell fate can be regulated by their relationship with other cells and by chemical and physical factors [1]. Cells are able to sense environmental mechanical signals and respond them by translating into biochemical responses. This process is known as mechanotransduction. Mechanical wave are sense by cell mechanoreceptors, that are transmembrane proteins that link with the cytoskeleton [2]. Once the mechanoreceptor receives the mechanical stimuli lead to the activation of different signaling pathways with finally rule cell fate, including quiescence, cell adhesion, proliferation, migration, differentiation, or apoptosis [3]. Hence, ultrasound, as mechanical stimuli, has the potential to regulate cell behavior.

Ultrasound has been widely used in biomedicine for more than fifty years—both as a safe and non-invasive diagnostic tool for real-time imaging (no radiation is emitted) and, more recently, as a surgical or therapeutic modality for various disorders or diseases (bone fractures, cancer and kidney stone ablation, among others) [4–6]. The breadth of practical applications of ultrasound waves are due, in part, to the ability to alter their properties depending on the parameters chosen. Indeed, new applications for ultrasound are continually evolving not only in the biomedical field but also in others such as the food industry [7]. Ultrasound can be used also for improve stem cell delivery and survival due to offers real-time guidance. Nowadays multimodal approaches are being developed in combination with photoacoustic imaging and magnetic particle imaging [8,9].

Low-intensity pulsed ultrasound (LIPUS), a form of ultrasound transmitted transcutaneously as high frequency acoustic pressure waves, has been approved for over two decades for bone fracture healing [10–12]. Not only has been continued the study their effects on osteogenic/bone repair [13,14], but also its study has been extended to new areas. Its use in soft tissue regeneration has drawn attention to potentially important novel properties including the stimulation of cell proliferation [15,16], migration [17,18] and angiogenesis [19,20]. Three major parameters for LIPUS are intensity, frequency and exposure time: typical parameters used are an ultrasound carrier frequency of 1.5 MHz, power intensity of 30 mW/cm^2 and daily duration of 20 min. Nevertheless, a range of intensity levels has been reported *in vitro*, from 0.03 to 0.1 W/cm^2 SATA (spatial average-temporal average) [21]. Using these parameters, the heat and cavitation risk is considered negligible [22]. Most if not all physiotherapy clinics have a conventional therapeutic ultrasound device, whereas a LIPUS device, for example the Exogen 2000+ (Smith & Nephew Inc.), is less common and considerably more expensive. Accordingly, the use the lower intensities of conventional therapeutic ultrasound devices might be an economical alternative to obtain LIPUS-like effects.

Mesenchymal precursors (MPs) are adult stem cells present in virtually every organ and are characterized by their ability to differentiate into various mesenchymal cell lineages. They are relatively easy to obtain from many cell depots and are endowed with important therapeutic properties including immunomodulatory potential and secretory and migratory functions [23–25]. Accordingly, they have a high potential to be used in regenerative/reparative processes. However, a limitation for their use as a therapy is their propensity to remain at the site of injection and their lack of migration to sites of damage, which drives the development of new strategies to overcome these challenges [26].

Due to the great potential of LIPUS for chronic skin wound healing, activation of fibroblast proliferation and migration [27], and production of extracellular components [28] such as collagen [29,30], we aimed to study whether ultrasound waves generated by a conventional device, at the lowest intensity setting, could reproduce these functions in skin mesenchymal precursors (s-MPs).

Material and methods

Isolation and expansion of mesenchymal precursors

Mice were maintained and used in accordance with the National Institutes of Health Animal Care and Use Committee. Protocols were approved by the Research Ethics Committee (CEI) of CNIC (Centro Nacional de Investigaciones Cardiovasculares). Mice were sacrificed by CO2 chamber. Human samples skin explants were obtained after esthetic ear surgery conformed to the principles set out in the WMA Declaration of Helsinki and the NIH Belmont Report. Protocols were approved by the Health Sciences Research Committee of Universidad Europea de Madrid with reference number CIPI/069/17. The isolation of s-MPs was performed using the explant technique described previously [31]. Skin explants from adult mice and adult humans were collected and dissected into 1–2 mm pieces. The tissue explants were placed in the center of 24-plate wells with the well contours coated with Matrigel ™ (BD Biosciences, Franklin Lakes, NJ, USA). Explant culture medium, referred to as complete medium, consisted of Dulbecco's modified Eagles's medium (DMEM) supplemented with 10% fetal bovine serum (both from Sigma-Aldrich, St Louis, MO, USA), 105 U/mL penicillin/streptomycin, 2 mM L-glutamine and 10 mM Hepes (all from Lonza, Basel, Switzerland). Cultures were maintained for several days at 5% CO_2/95% air atmosphere at 37˚C and, after 1 week, cells appeared around the explant. Cell expansion was performed on gelatin-free culture plates. Studies were performed using cells from passage 10 to 20. Cells were characterized by flow cytometry as follows: human cell populations were positive for CD105 and negative for CD34; murine cell populations showed a variable expression of CD34 and Sca-1. Both populations were positive for CD44 and negative for CD31 and CD45, confirming that they are non-hematopoietic mesenchymal precursors. The experiments were done with two independent cell populations from both human (H1 and H2) and mouse (M1 and M2) samples. However, for RNA-sequencing we used four human cell populations, to strengthen the biological interpretation of the results.

Ultrasound application (low-intensity pulsed therapeutic ultrasound)

Application of ultrasound (therapeutic LIPUS) to cells was performed using the Medisound 3000 device (Globus, Codognè, Italy), which is approved by the EU for use in hospitals and physiotherapy clinics. A total of 1.5×10^4 cells were seeded in each well of a 24-well plate and were maintained for 24 h in the humidified incubator before stimulation. Application of LIPUS to s-MPs was performed using the following parameters (Fig 1): 100 mW/cm^2 intensity (lowest available power) and 3 MHz frequency. The LIPUS protocol consisted of 20 minutes each day with an ultrasound pulsed at 20% (1:4) at 1000 Hz, for three consecutive days. LIPUS was applied outside of the incubator at room temperature, with control cultures treated identically (without LIPUS). Once the daily application was completed, the cells were returned to the incubator. On day four cells were trypsinized and expanded to ~1×10^6 cells for experiments. All experiments were carried out five days after the final LIPUS application, which was necessary to expand the cells (Fig 1).

Proliferation assay–cell counting

For cell counting experiments, 1×10^4 cells were seeded in each well of a 24-well plate and counted over three days. The results were expressed as a proliferation curve representing the total number of cell present on the plate each day.
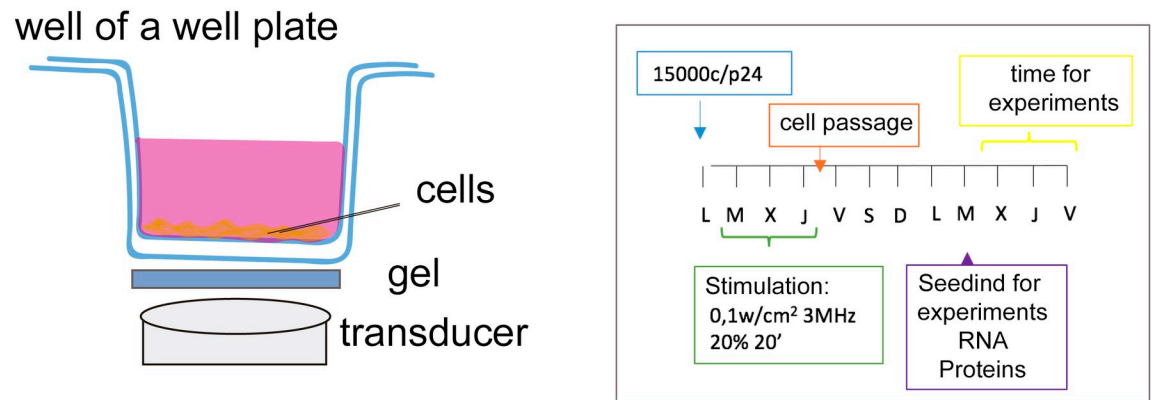
Fig 1. Scheme of the ultrasound application and the experimental design. The application of LIPUS was performed with a gel between the transducer and the bottom of the plate where the cells are attached. The experiments were conducted 5 days after the final application of LIPUS. Ultrasound attenuation within a polystyrene standard culture plate (1.2 mm) has been described as not significant (less than 0.3 dB or 4% over the frequency range from 1 to 3 MHz) [32].

https://doi.org/10.1371/journal.pone.0246261.g001

Proliferation assay–bromodeoxyuridine incorporation

The bromodeoxyuridine (BrdU) assay (Merck KGaA, Darmstadt, Germany) was used for proliferation analysis, which is based on the incorporation of the thymidine analog BrdU into DNA strands during replication. Briefly, 5×10^3 cells were seeded in each well of a 96-well plate. The next day, BrdU (1:2000 dilution) was added to the culture and cells were maintained for 24 h. Cells were then fixed and washed and incorporated BrdU was detected with an anti-BrdU antibody (1:100, 1 h incubation at room temperature), which was visualized with an HRP-conjugated secondary antibody (1:1000, 30 min at room temperature). Finally, after washing, the chromogen substrate was added for 30 min in the dark for the development of the peroxidase reaction. Once the STOP solution was added, the optical density was read in a spectrophotometer (SPECTROstar^{Nano}; BMG LABTECH, Aylesbury, UK) at 450 nm.

Fluorescence microscopy

Cells (2.5×10^4) were plated on 0.1% gelatin-coated coverslips in a 24-well plate and were maintained in culture for 24 h. Then, coverslips were washed with phosphate buffered saline (PBS), fixed with 4% paraformaldehyde for 15 min, and blocked with 1% goat serum for 1 h at room temperature. Primary antibodies used were rabbit anti-tubulin (1:100 concentration; Abcam, Cambridge, UK) and phalloidin-TRITC (1:100 dilution; Sigma-Aldrich). Antibody staining was carried out in antibody dilution buffer overnight at 4°C. For tubulin staining, after washing with PBS, a goat anti-rabbit Alexa488 secondary antibody was added (1:400 dilution; Invitrogen, Life Technologies, Carlsbad, CA, USA) for 1 h in the dark at room temperature. Coverslips were co-stained with DAPI (300 nM; Sigma-Aldrich) for 10 min at room temperature and mounted with ProLong Antifade reagent (Invitrogen) on glass slides. Images were observed with a Leica DM2000 LED (Leica Microsystems, Wetzlar, Germany).

Wound-healing assay

To evaluate collective migration, we used the wound-healing assay. Confluent s-MP cultures were scratch-wounded with a sterile micropipette tip, washed with PBS to remove cellular debris, and replenished with complete medium. Cells were maintained in culture and images were captured at different times using a Motic AE31 microscope (Motic, Hong Kong, China).

The calculation of the wound area was performed with ImageJ software (Bethesda, MD, USA). The results were expressed as a percentage of wound closure.

Transwell migration assay

To evaluate individual migration, we used Transwell chambers (Corning Inc., MA, USA) with 6.5 mm-diameter permeable membranes and 8-μm pore size filters. Murine (2×10^4) and human (5×10^4) s-MPs were plated in 80 μl of medium in the upper chamber of the Transwell chamber (placed on 24-well plates) and complete culture medium was placed in the lower chamber. After 24 h, chambers were fixed with 4% glutaraldehyde for 2 h and then stained overnight with 1% toluidine blue (both from Sigma-Aldrich). Cells on the lower side of the membrane were visualized with a Motic AE31 microscope and counted in five randomly-selected 10× fields using ImageJ software (Bethesda, MD, USA). The results were expressed as migrated cells per field.

Transwell invasion assay

Invasion assays were performed following the same protocol as the Transwell migration assays, but membranes were coated beforehand with 1% gelatin in PBS for 1 h at 37˚C.

Quantitative PCR

Total RNA was extracted from s-MPs using the Easy-spin Total RNA Extraction Kit (iNtRON Biotechnology, Sangdaewon-Dong, South Korea) and its concentration was quantified in a spectrophotometer (ND1000 NanoDrop, Thermofisher Scientific, Rockford, IL, USA). RNA was reverse-transcribed to cDNA using PrimeScript™ RT Master Mix (TAKARA Bio. Inc., Kusatsu, Japan). Quantitative PCR (qPCR) was performed using SYBER® Green PCR Master Mix (Premix Ex Taq™, TAKARA Bio. Inc.) on the CFX96 Touch Deep Well™ Real-Time PCR Detection System (Bio-Rad Laboratories, Richmond, CA, USA). Thermal cycling parameters were as follows: first step of 94˚C for 10 min, then 40 cycles of 94˚C for 15 s and the primer-specific annealing temperature for 1 min (56˚C). The last step was the melting curve analysis. qPCR was performed using the primers in Table 1.

Western blotting

Cell lysates were extracted and lysed directly on ice using Laemmli buffer. Lysates were resolved by electrophoresis using 12% SDS-PAGE and proteins were transferred to nitrocellu-lose membranes for immunodetection. Membranes were blocked with 5% nonfat milk in PBS for 1 h at room temperature and subsequently incubated overnight at 4˚C with a 1:1000 dilu-tion of the primary antibody (β1laminin, β1integrin, βactin; Abcam, Cambridge, UK), fol-lowed by a quick wash in PBS containing 0.1% Tween-20 and detection with the appropriate

Table 1. Primers for qPCR.

Gene name	Forward	Reverse
GAPDH	AATGCATCCTGCACCACCAA	GTGGCAGTGATGGCATGGAC
ROCK1	TGCCATGTTAAGTGCCACAG	AGGGGAAGCACGAACAAAAC
COL1A1	TGATGGGATTCCCTGGACCT	TCCAGCCTCTCCATCTTTGC
TGFB1	CTGCTGACCCCCACTGATAC	GTGAGCGCTGAATCGAAAGC
LAMB1	AGGAGACTGGGAGGTGTCTC	GTCAGAGCCGTTACAGTGCT
ITGB1	GCCGCGCGGAAAAGATG	TGAATTTGTGCACCACCCAC

secondary antibody (anti-rabbit HRP). Blots were visualized with the ECL reagent using a ChemiDoc XRS+ system (Bio-Rad Laboratories) and relative intensity was quantified by densitometry using ImageJ software (Bethesda, MD, USA).

RNA-sequencing

RNA-sequencing library preparation and sequencing of the human cell samples was carried out by STABVida Lda (Caparica, Portugal). RNA integrity was checked on a Bioanalyzer 2100 (Agilent Technologies, Santa Clara, CA, USA). The Kapa Stranded Total RNA and Ribo-Zero Library Preparation Kit were employed for library construction, and sequencing was performed using the HiSeq 4000 Illumina Platform with 2×150 bp paired end reads. The bioinformatics analysis of the generated raw sequence data was carried out using CLC Genomics Workbench 11.0.1. Further quality control was performed by principal component analysis (PCA), hierarchical clustering (considering Manhattan distance), and heat map analysis. Differential expression was then calculated using multi-factorial statistical analysis based on a negative binomial model that used a generalized linear model approach influenced by the multi-factorial EdgeR method [33]. The differentially expressed genes were filtered using standard conditions [33], a p-value less than 0.05 and fold change over 2 or under -2. Raw data in fastq format are available with the accession number PRJNA662884 in the NCBI Biosample database (https://www.ncbi.nlm.nih.gov/sra/PRJNA662884).

Data analysis

Statistical analysis and graphical representation of the results was performed using GraphPad Prism software (GraphPad Software Inc., San Diego, CA, USA). Values are expressed as mean ± standard deviation (SD) from 3 independent experiments. Data were checked for normality using the D'Agostino-Pearson test. Comparisons between groups were performed with one-way or two-way analysis of variance (ANOVA). The multiple comparisons test used for one-way ANOVA was Bonferroni's and for two one-way ANOVA we used Tukey's. Student's t test was used when there was only one variable to consider. The specific analysis used is specified in the figure legends. Data was considered significantly different when $P < 0.05$; $^*P < 0.05$; $^{**}P < 0.01$; $^{***}P < 0.001$.

Results

Low-intensity ultrasound application procedure

Ultrasound exposure (Medisound 3000) was performed on cells adhered to tissue culture plates, at low confluence ($1.5×10^4$) and prior to experimental testing. We had previously discarded the application of ultrasound on suspended cells (as mechanotransduction occurs with adhered cells) or directly during experimental testing (ultrasound application would not be homogeneous). Attached cells were stimulated at 100 mW/cm^2 with 3 MHz for 20 min, and a 20% duty-cycle during 3 days [17]. As shown in Fig 2, cells receiving the ultrasound application were morphologically indistinguishable from control cells. As a positive control of US stimulation, the increase of the intensity to 1 W/cm^2 caused the death of the cells (S1 Fig).

Low-intensity ultrasound stimulation does not produce noticeable changes in cytoskeleton organization

To assess whether the LIPUS stimulation protocol resulted in changes to the organization of the cytoskeleton in s-MPs, we analyzed the distribution of F-actin (actin filaments) and β-tubulin (microtubules) using fluorescence immunocytochemistry. Stimulated s-MPs from
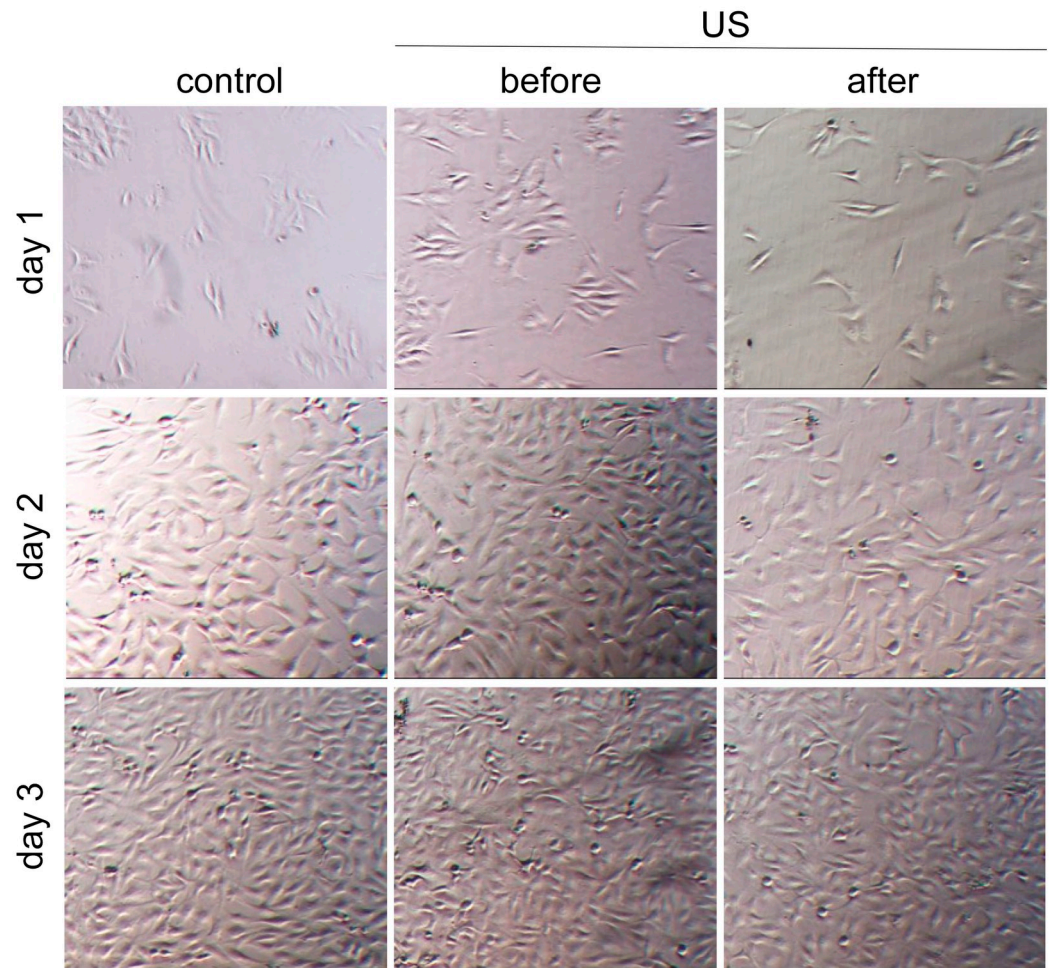
Fig 2. Application of LIPUS. Representatives phase contrast images of human s-MPs showing control cells and LIPUS-stimulated (US) cells before and after consecutive treatment during 3 days.

human and mouse had a comparable morphology to respective controls (Fig 3), with evident actin filaments and microtubules. No cytoskeletal reorganization could be detected (clusters or other structures) in the stimulated cells. Overall, the LIPUS protocol used with the selected parameters appears not to cause any manifest structural changes to cell morphology and the cytoskeleton.

Low-intensity ultrasound stimulation does not affect cell proliferation

To question whether the LIPUS stimulation protocol impacted cell proliferative potential, we performed both BrdU incorporation and manual cell counting. The results of both assays indicated no differences in the proliferation rate of cells subjected to LIPUS stimulation when compared with control cells, with similar results for murine and human s-MPs (Fig 4).

Low-intensity ultrasound stimulation does not affect migration capacity

Next, to evaluate whether the LIPUS protocol impacted the capacity of s-MPs to migrate, an important attribute of MPs, we performed several migration-based assays. We first utilized the scratch wound-healing assay to study collective two-dimensional cell migration. No significant
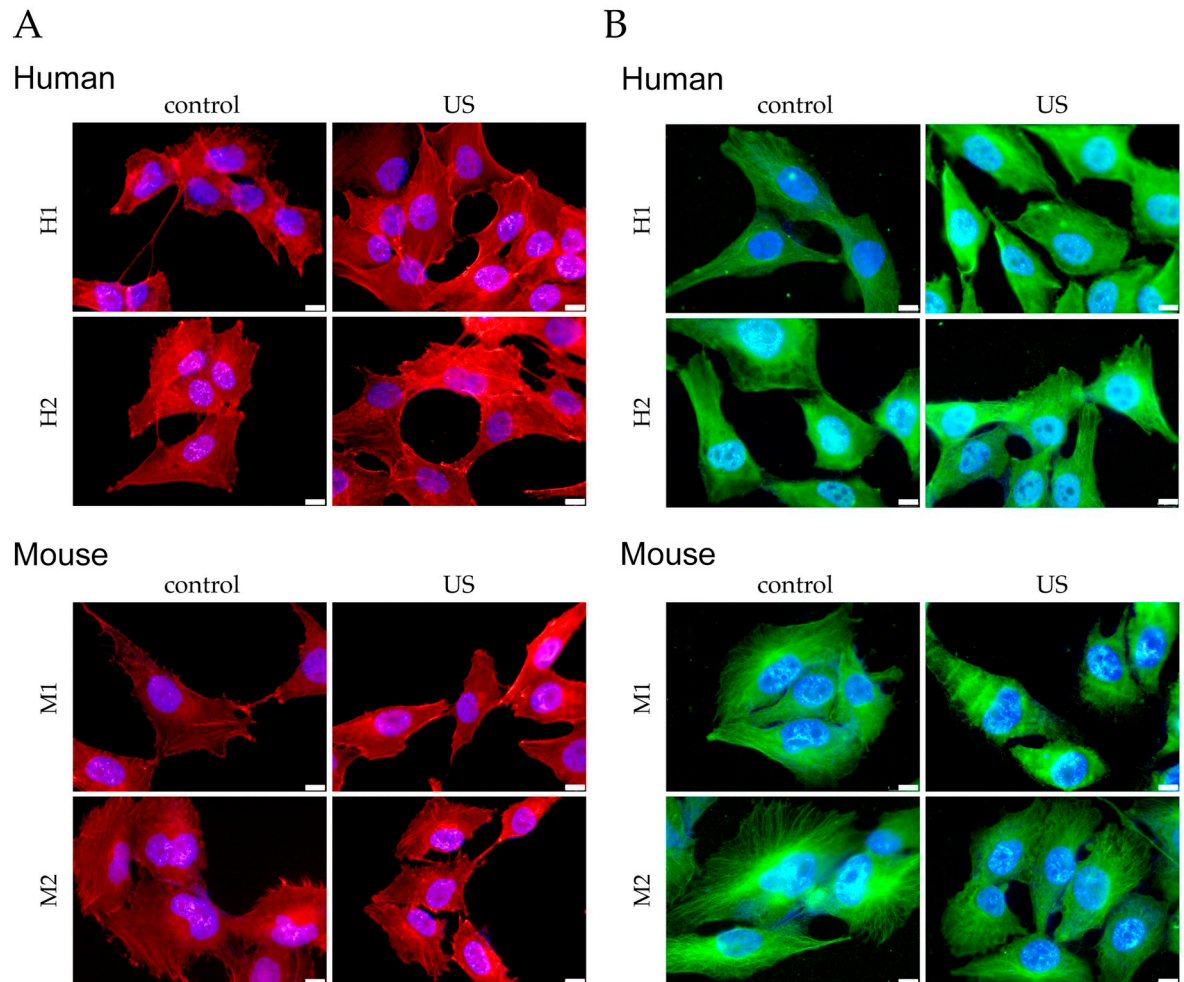
Fig 3. Application of LIPUS does not affect the cytoskeletal organization of s-MPs. Control cells and cells stimulated with LIPUS (US) for 3 days were stained with (A) phalloidin-TRITC to visualize F-actin (red) and (B) β-tubulin to visualize microtubules (green). Nuclei were counter-stained with DAPI (blue). Shown are two independent samples of mouse (M1 and M2) and human (H1 and H2) s-MPs. Images are shown at a magnification of 63×, scale bar 10 μm.

https://doi.org/10.1371/journal.pone.0246261.g003

differences in wound closure were observed between human control and LIPUS-stimulated s-MPs (Fig 5). With respect to murine s-MPs, wound closure occurred faster in LIPUS-stimulated cells than in control cells, and this was significant for one of the two independent s-MP populations; however, the increase was modest (Fig 5).

We also performed a migration assay using Transwell chambers, which were used to assess individual migration through a porous membrane. Of note murine s-MPs had a considerably greater migratory capacity than human counterparts (Fig 6). Similar to the results of the scratch assay, however, no significant changes in migration were observed between human control and LIPUS-stimulated s-MPs (Fig 6). With respect to murine s-MPs, again migration occurred faster in LIPUS-stimulated cells than in control cells, and this was significant for one of the two independent s-MP populations (Fig 6).

We repeated the Transwell migration assays using membranes coated with 1% gelatin to create a three-dimensional matrix to assess invasion. Similar to the standard Transwell assay, we observed that murine s-MPs migrated faster than human counterparts (Fig 7). However, there were no differences in the invasion capacity between control and stimulated cells, with
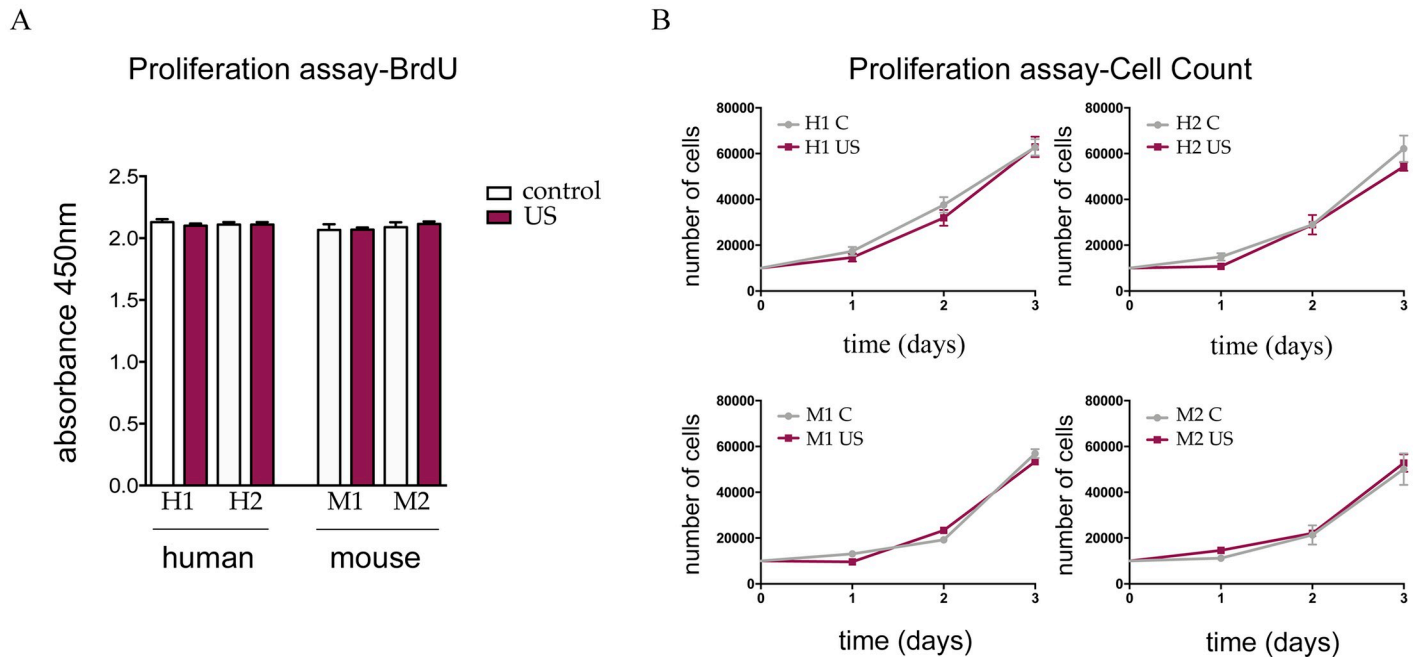
A

Proliferation assay-BrdU

B

Proliferation assay-Cell Count

Fig 4. Application of LIPUS does not modify the proliferation capacity of s-MPs. (A) Cell proliferation was evaluated by BrdU incorporation. Data are shown from a representative experiment out of three performed and denote mean ± SD. No significant differences were found (Student's t-test). (B) Cell proliferation was calculated by cell counting. Data are shown from a representative experiment out of three performed and denote mean ± SD. No significant differences were found (two-way ANOVA with Tukey's multiple comparisons test). Shown are two independent samples of mouse (M1 and M2) and human (H1 and H2) s-MPs under control conditions or treated with ultrasound (US).

https://doi.org/10.1371/journal.pone.0246261.g004

the exception of one of the human s-MP samples, in which migration was modestly but significantly greater.

Overall, the results of the migration assays strongly suggest that, at the parameters used, ultrasound stimulation does not improve the migration capacity of s-MPs.

Low-intensity ultrasound does not modify the expression of ROCK1, COL1A1, TGFB1, LAMB1 and ITGB1

We next analyzed the expression status of several molecules related to mechanotransduction process and to the molecular mechanism of action of LIPUS: ITGB1 (integrin β1), a cellular receptor involved in mechanotransduction; ROCK1 and TGFB1 (transforming growth factor β1), important for cell signaling and function; and LAMB1 (laminin β1) and COL1A1 (type I collagen), important as extracellular matrix components [18,34–37]. RNA and proteins were extracted 5 days after the ultrasound application, and were used for qPCR and western blotting analysis, respectively. Results showed that the mRNA expression of *ROCK1*, *COL1A1*, *TGFB1*, *LAMB*, and *ITGB1* remained unchanged after the ultrasound treatment, both in murine and human s-MPs (Fig 8). Nor were changes detected in the expression of the genes that code for cytokines or one of their receptors: *CXCL12*, *CCL2* and *CXCR4* (S2 Fig).

RNA-seq

Given the above negative results for the comparison of gene/protein changes with respect to ultrasound application, we performed a more in-depth analysis of gene expression by RNA-seq. Analysis was performed with four different samples of human cells (controls *versus*

Migration assay-*Wound Healing*
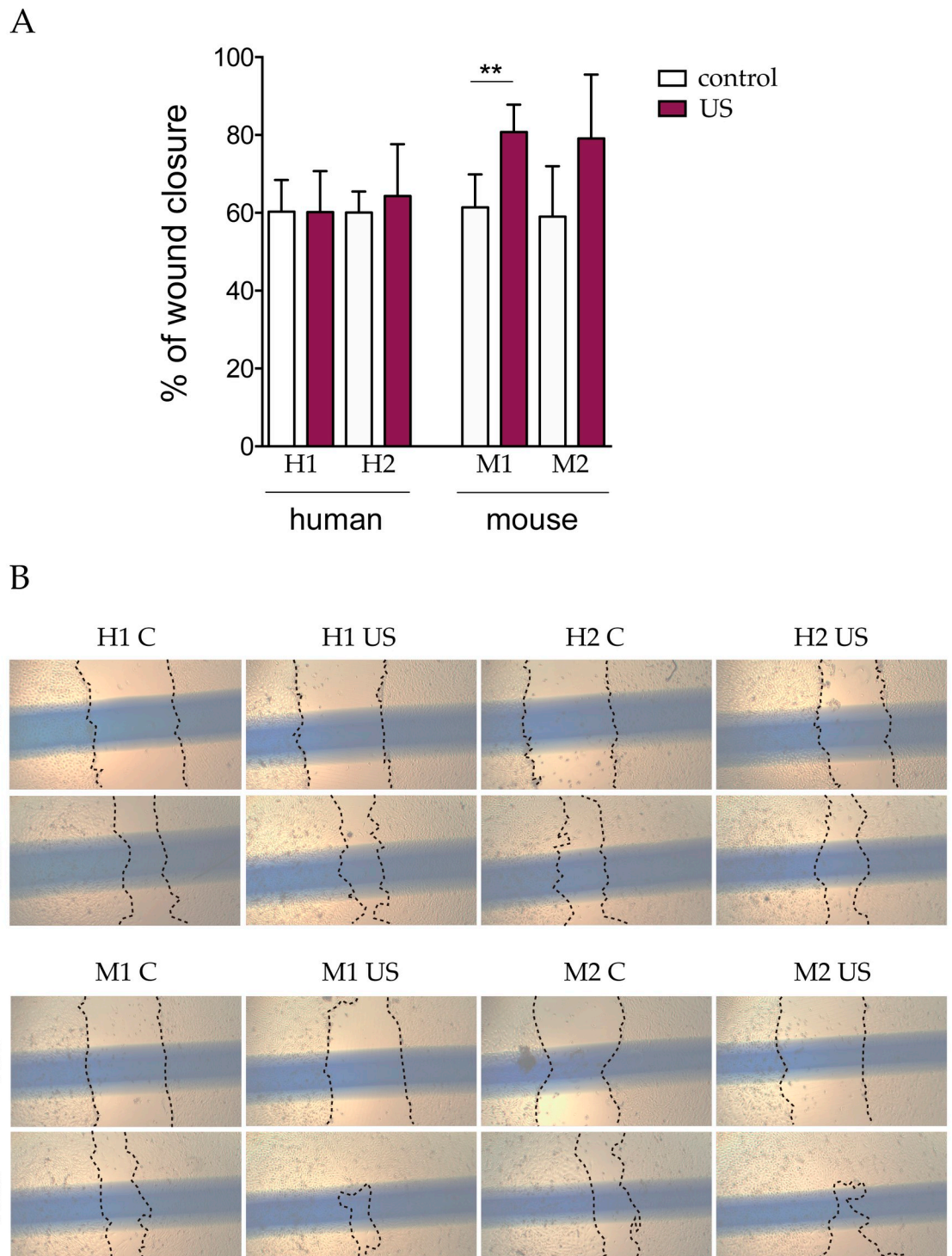
Fig 5. Wound healing migration assay. (A) Data are shown from a representative experiment out of five performed and denote mean ± SD (quantification at 16 h). Statistical analysis was performed using Student's t test. **p < 0.01. (B) Representative images of the wound at time 0 h and 16 h after scratching. Shown are two independent samples of mouse (M1 and M2) and human (H1 and H2) s-MPs under control conditions or treated with ultrasound (US).

https://doi.org/10.1371/journal.pone.0246261.g005

Migration assay-*Transwells*

Fig 6. Transwell migration assay. (A) Data are shown from a representative experiment out of three performed and denote mean ± SD. Statistical analysis was performed using Student's t test. ***p < 0.001. (B) Representative images (10×) of the migrated cells. Shown are two independent samples of mouse (M1 and M2) and human (H1 and H2) s-MPs under control conditions or treated with ultrasound (US).
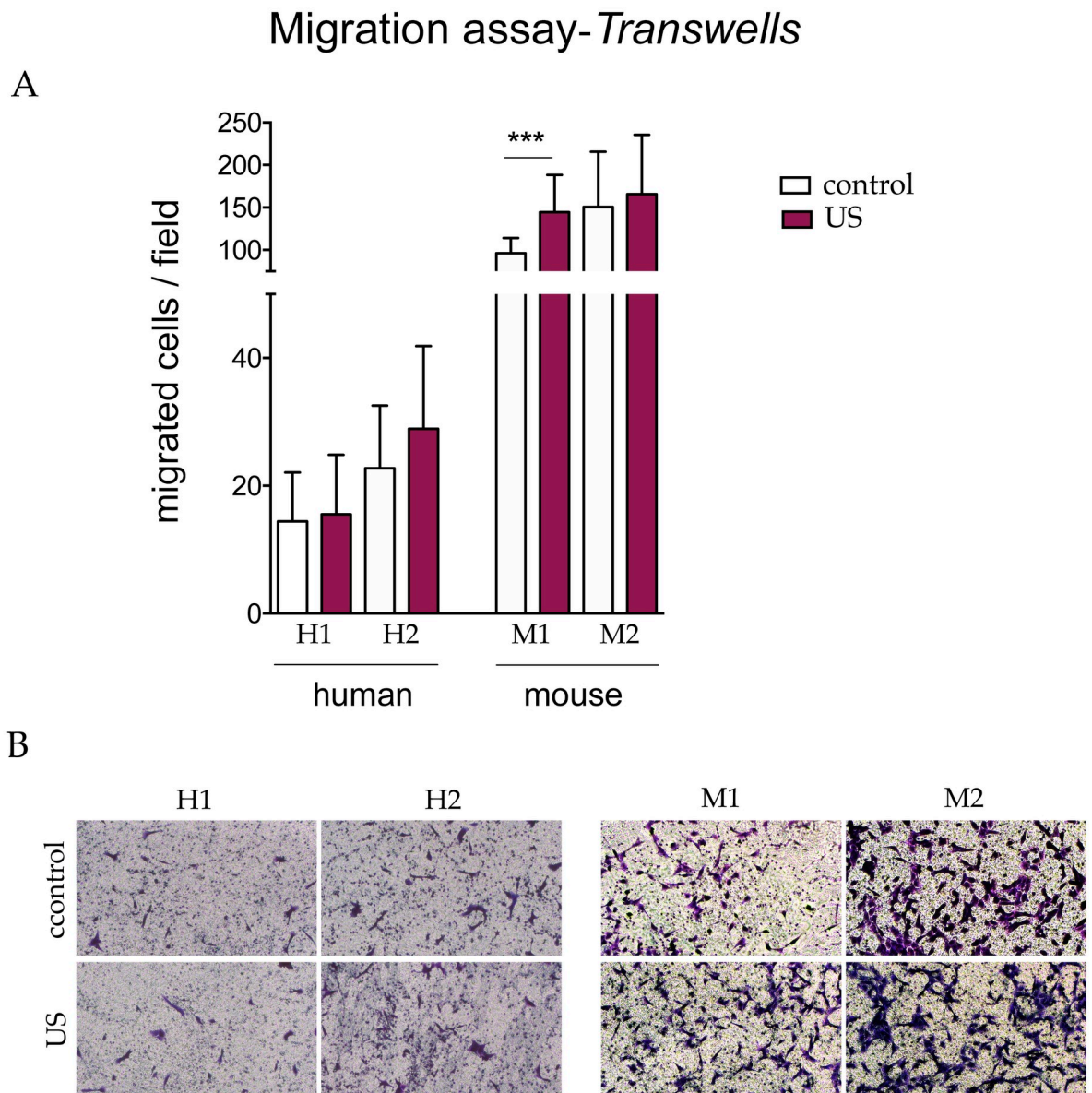
ultrasound). Surprisingly, but at the same time consistent with previous results, only 10 genes were differentially expressed by the ultrasound protocol, as shown by Volcano plot (Fig 9A).

Heat map analysis showed no overall change in expression patterns (Fig 9B). Of the 10 genes differentially expressed, 2 were upregulated by ultrasound and 8 were downregulated (Fig 9C). Interestingly, among the genes with an altered expression pattern, 5 genes encode for small nuclear RNAs (snRNAs) and 2 genes encode for proteins belonging to the nuclear pore complex.
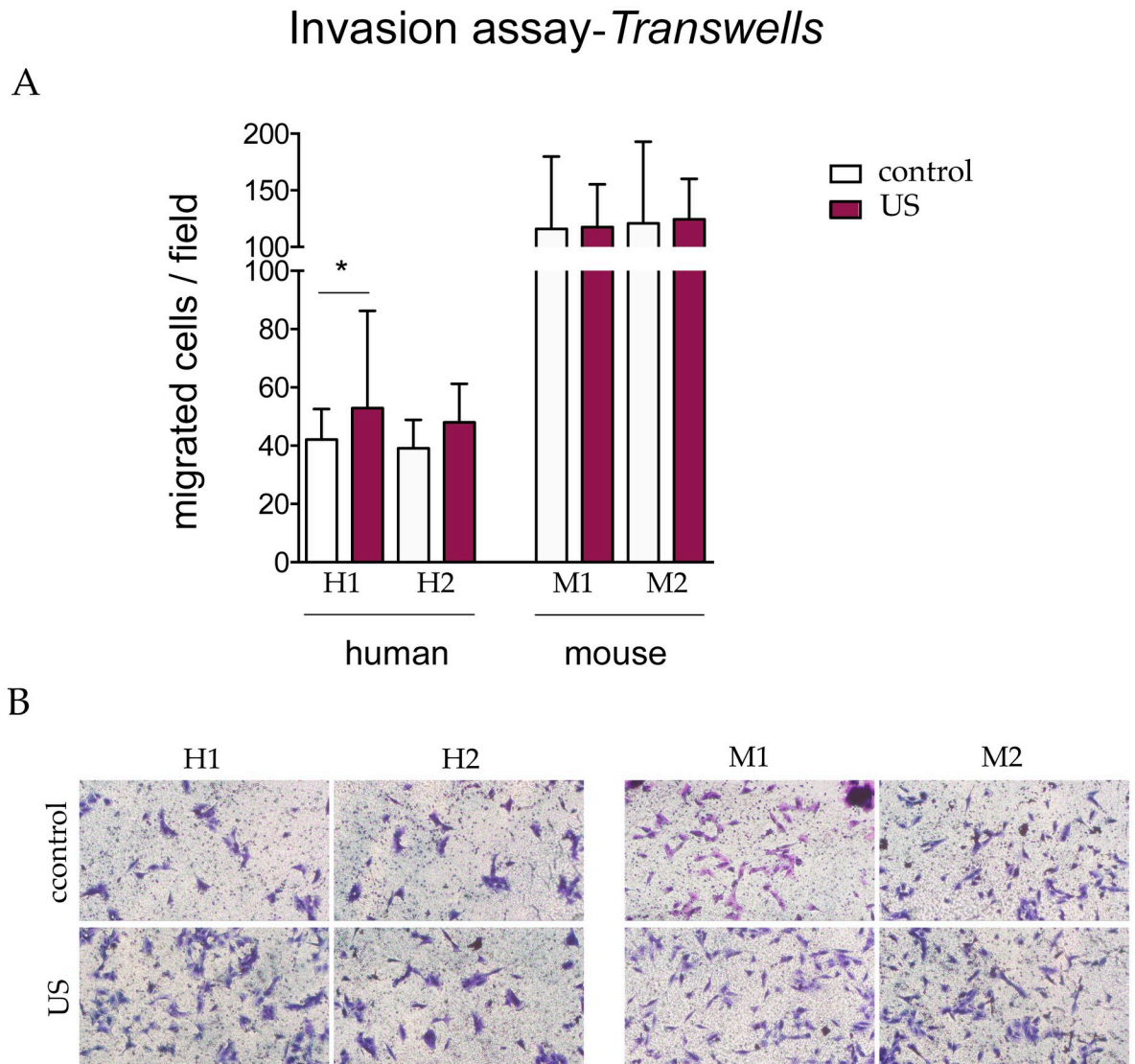
Invasion assay-*Transwells*

Fig 7. Transwell invasion assay. (A) Data are shown from a representative experiment out of three performed and denote mean ± SD. Statistical analysis was performed using Student's t test. *p < 0.05. (B) Representative images (10×) of the migrated cells. Shown are two independent samples of mouse (M1 and M2) and human (H1 and H2) s-MPs under control conditions or treated with ultrasound (US).

Discussion

Ultrasound has proven to have a range of biomedical and other applications. Focusing on the application of LIPUS in wound healing [30,38], by triggering the proliferation and migration of fibroblasts and the concomittant synthesis and deposition of extracellular matrix components, we sought to assess whether low-intensity ultrasound delivered by a conventional device could replicate the positive effects of LIPUS. The benefits of using conventional ultrasound devices are that they are approved by the European Union (for use in Europe) and are found both in hospitals and in physiotherapy clinics, thus negating the need to purchase specific LIPUS devices. Conventional ultrasound devices allow the adjustment of the ultrasound parameters to those within the range of LIPUS, and we used the lowest available intensity, 100 mW/cm^2 (from intensities up to 3000 mW/cm^2) in the present study. While the standard
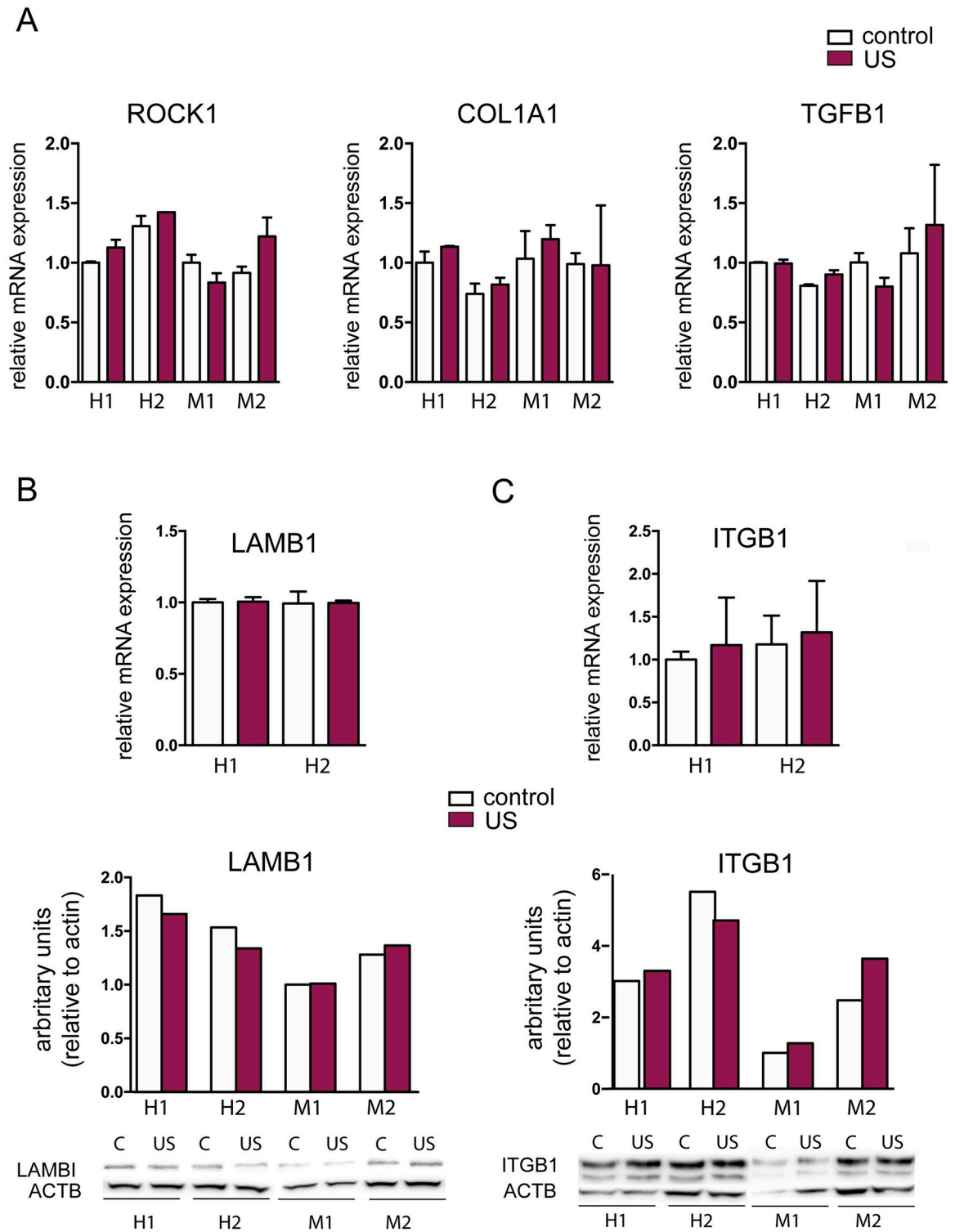
Fig 8. Gene and protein expression analysis. (A) Gene expression of *ROCK1*, *COL1A1*, *TGFB1*. Data are shown from a representative experiment out of three performed and denote mean ± SD. (B) Gene and protein expression of *LAMB1*, and *ITGB1*. Data are shown from a representative experiment out of three performed and denote mean ± SD. Statistical analysis was performed using one-way ANOVA with Bonferroni's multiple comparisons test. Shown are two independent samples of mouse (M1 and M2) and human (H1 and H2) s-MPs under control conditions or treated with ultrasound (US).

https://doi.org/10.1371/journal.pone.0246261.g008

Fig 9. RNA-seq results. (A) Volcano plot showing the 10 genes differentially expressed between control and ultrasound-stimulated (US) human s-MPs. (B) Heat map graph, where the red zones are correlate with upregulated genes and the blue zones with the absence of changes in expression. (C) Differentially expressed genes that fulfill the conditions to present a p-value under 0.05 and fold change over 2 or under -2.
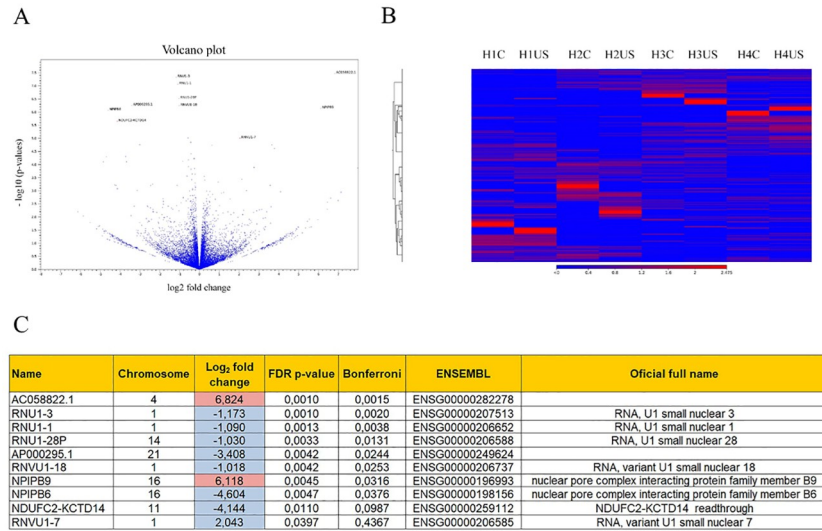
https://doi.org/10.1371/journal.pone.0246261.g009

parameters of LIPUS are well established (power intensity of 30 mW/cm^2, frequency of 1.5 MHz, 20% duty cycle), as they are the most often used, there are multiple references to studies with small variations of these parameters, although remaining pulsed ultrasound characterized by its low intensity. Several studies using intensities greater than 30 mW/cm^2 have reported beneficial results in different settings. In rats, the use of LIPUS at 100 mW/cm^2 accelerates fracture repair [22]. Likewise, an intensity of 83 mW/cm^2 induced cardiac differentiation and increased the malleability and mobility of cardiac mesoangioblasts [18]. Much greater intensities (100–1500 mW/cm^2) have been used on induced pluripotent stem cell-derived neural crest stem cells, which provoked an increase in cell viability, proliferation and neural differentiation [39]. It has been reported that an increase in the time of treatment increases the effectiveness of LIPUS, in a dose-dependent manner [40]. Furthermore, numerous studies have used frequencies other than 1.5 MHz, of which the more typical is 1 MHz [41–43] or 3 MHz [16], both of which are available from conventical therapeutic devices. Closer to our present study, LIPUS intensities of 160/240 mW/cm^2 and frequency of 3 MHz were used successfully to promote cell proliferation and wound closure in epithelial cells [44]. Given this evidence, we stimulated mesenchymal precursors from mouse and human skin with ultrasound at 100 mW/cm^2, 3 MHz, 20% duty-cycle for 20 min for three consecutive days, and cell migration and other properties were analyzed. Gross morphological analysis of stimulated s-MPs indicated that the protocol was not detrimental, as morphology was similar to control cells throughout the three-day application. However, it has also been described that LIPUS can induce apoptosis when higher intensities are applied [3,45,46] as occurs when we used 1 W/cm^2 intensity as a positive control for ultrasound stimulation. Therefore, LIPUS could be a potential tool for the treatment of some cancers [47].

Ultrasound is a mechanical stimulus that is transmitted to the cell by mechanotransduction process. This occurs through different mechanoreceptors (transmembrane proteins) that can be integrins, stretch-activated ion channels (piezo mechanosensitive ion channels) [48–50] which act as mediators between the cytoskeleton and the extracellular matrix [51]. Because ultrasound is known to reorganize the cellular cytoskeleton [18,52], we examined the

morphology and cytoskeleton of stimulated s-MPs, particularly actin filaments and microtubules, finding no changes in their distribution.

We next examined cellular proliferation capacity, as this has been shown to be affected by ultrasound stimulation in some studies [15,16]. However, no differences were found between unstimulated and ultrasound-stimulated cells.

To investigate whether the ultrasound protocol could improve cellular migration ability, as previously reported [17,18], and which is a key attribute for enhanced therapeutic potential, we used three complementary assays to examine different types of migration. Overall, none of the three assays showed changes in the migration capacity of s-MPs after ultrasound stimulation, although some modest, but significant, changes were occasionally observed. Of note, however, murine s-MPS had a greater capacity to migrate in Transwell assays than their human counterparts.

Consistent with the previous results, an analysis of different genes and proteins whose expression has been previously linked to proliferation (TGFB1), cytoskeletal reorganization (ITGB1) and migration (ROCK) induced by ultrasound stimulation [18,35,53] revealed no changes in their expression.

Finally, the RNA-seq analysis showed that the ultrasound protocol used in human s-MPs triggered very minor changes in gene expression, and only 10 genes were affected by the treatment. Interestingly, among these differentially expressed genes, 5 genes encode for snRNAs and 2 genes for proteins belonging to the nuclear pore complex. snRNA biogenesis is linked to specialized nuclear suborganelles termed Cajal bodies [54]. snRNAs are involved in the formation and function of the spliceosome [55] and Cajal bodies also act as processing centers for ribonucleoprotein assembly, ribosome biogenesis and telomere maintenance [56]. Variations in the proteins associated with Cajal bodies have been reported following changes in integrins upon mechanical stimuli, indicating that forces on the cellular surface can be transmitted to the nucleus *via* cytoskeletal components [54,57]. Integrins and cadherins are physically coupled to the cellular cytoskeleton, inducing transmission of signals along the proteins. Further, F-actin filaments are joined to microtubules and intermediate filaments, which also connect with nuclear pore complexes, offering an explanation for the relationship between nuclear pores and the cytoskeleton [58]. Our results showing changes in the expression of snRNAs and in proteins of the nuclear pore complex could be a good indicator that ultrasounds are reaching the s-MPs including the nucleus.

While it would appear that ultrasound is safe for use in MPs, which is encouraging, the parameters used in the present study were not optimal to activate certain signaling routes. Of all the parameters that characterize ultrasound waves, intensity is the most relevant, which represents the passage of energy in a given area. The time and duty cycle that we used are standard, whereas the changes introduced were for frequency and intensity. Frequency indicates the number of times a particle experiencing a complete compression and rarefaction cycle in one second and is related to the capacity of the waves to penetrate a body or surface [59]. The use of frequencies of 1.5 MHz or 3 MHz both result in an increase of bone remodeling in rats, with no significant differences between them [60]. However, there is evidence to suggest that 100 mW/cm^2 might not be the most appropriate intensity to apply to cells. For example, osteoclast activity decreased significantly when 100 mW/cm^2 was employed instead of 30 mW/cm^2 [61]. Also, the use of 150 mW/cm^2 did not further enhance fracture healing in rats when compared with 30 mW/cm^2 [62], and settings of 30 and 120 mW/cm^2 in murine osteoblastic cells had different effects on mineralization processes in vitro [63]. In contrast to power settings above 30 mW/cm^2, intensity values below this can still promote osteogenesis [64]. These findings might explain our results and indicate that at the level of cell stimulation, the use of

traditional conventional devices with intensities of 100 mW/cm^2 would not be the most appropriate conditions, at least in our cell population.

Limitations and further studies

In our study, for ultrasound parameters selection we have the inherent limitation of the chosen device (physiotherapy ultrasound equipment). We are not able to assess intensities bellow 100mW/cm^2 and frequencies of 2 or 4 MHz. The use of ultrasound has great potential for several fields of biomedicine. However, it is of great importance to investigate and properly define the specific parameters that control cell fate. Thus, it would be convenient to analyze a range of intensities-frequencies and perform RNA-seq and protein from the day after the stimulation and check the time evolution to improve the knowledge of the stimulation process and how it affects the cells trough the time. It would also be interesting to study the effect of ultrasound on 3D or spheroid-cultured cells in order to better simulate tissue organization in organisms. Although ultrasound is a promising field, much more research is needed to advance in its translation into the clinical practice.

Conclusions

The final aim of the study was to evaluate the possibilities of physiotherapy ultrasound equipment for skin regeneration. Ultrasound stimulation of s-MPs with this device had no detrimental effects on cell viability; however, the functional properties of the cells studied did not improve, although we believe that the cells received and responded to the ultrasound signal due to the induction of snRNAs and proteins of the nuclear pore complex that are the result of the mechanotransduction process to the nucleus. In conclusion, the use of physiotherapy equipment with LIPUS parameters fails to improve skin precursors capacities and evidence the importance of standardizing ultrasound application parameters and methods.

Supporting information

S1 Fig. 1 W/cm^2 ultrasound application. Representatives phase contrast images of human and mice s-MPs showing the effects of the stimulation using 1 W/cm^2 of intensity.
(TIF)

S2 Fig. Gene expression level of *CXCL12*, *CCL2* and *CXCR4*. Graph that represent gene expression of *CXCL12*, *CCL2* and *CXCR4*. Similar results were obtained for protein expression analysis of laminin β1 and integrin β1 by western blotting (Fig 8). Thus, the ultrasound application using the selected parameters does not trigger modifications in the expression of LIPUS-related mechanostransduction molecules in s-MPs.
(TIF)

S1 Raw Images.
(PDF)

Acknowledgments

We thank Dr. Kenneth McCreath for critical reading of the manuscript.

Author Contributions

Conceptualization: Beatriz de Lucas, Aurora Bernal, Beatriz G. Gálvez.

Data curation: Beatriz de Lucas, Beatriz G. Gálvez.

Formal analysis: Aurora Bernal.

Funding acquisition: Beatriz G. Gálvez.

Investigation: Beatriz de Lucas, Laura M. Pérez, Beatriz G. Gálvez.

Methodology: Beatriz de Lucas, Laura M. Pérez, Aurora Bernal.

Supervision: Aurora Bernal, Beatriz G. Gálvez.

Writing – original draft: Beatriz de Lucas, Aurora Bernal.

Writing – review & editing: Laura M. Pérez, Beatriz G. Gálvez.

References

1. de Lucas B, Pérez LM, Gálvez BG. Importance and regulation of adult stem cell migration. J Cell Mol Med [Internet]. 2017 Dec 7 [cited 2018 Aug 31]; 22(2):746–54. Available from: http://www.ncbi.nlm.nih.gov/pubmed/29214727 https://doi.org/10.1111/jcmm.13422 PMID: 29214727

2. Vogel V. Mechanotransduction involving multimodular proteins: Converting force into biochemical signals [Internet]. Vol. 35, Annual Review of Biophysics and Biomolecular Structure. Annu Rev Biophys Biomol Struct; 2006 [cited 2020 Nov 19]. p. 459–88. Available from: https://pubmed.ncbi.nlm.nih.gov/16689645/ https://doi.org/10.1146/annurev.biophys.35.040405.102013 PMID: 16689645

3. de Lucas B, Pérez LM, Bernal A, Gálvez BG. Ultrasound therapy: Experiences and perspectives for regenerative medicine [Internet]. Vol. 11, Genes. MDPI AG; 2020 [cited 2020 Nov 19]. p. 1–21. Available from: /pmc/articles/PMC7563547/?report=abstract https://doi.org/10.3390/genes11091086 PMID: 32957737

4. Harrison A, Lin S, Pounder N, Mikuni-Takagaki Y. Mode & mechanism of low intensity pulsed ultrasound (LIPUS) in fracture repair [Internet]. Vol. 70, Ultrasonics. Elsevier B.V.; 2016 [cited 2020 Sep 25]. p. 45–52. Available from: https://pubmed.ncbi.nlm.nih.gov/27130989/

5. Zhang L, Zhang W, Orsi F, Chen W, Wang Z. Ultrasound-guided high intensity focused ultrasound for the treatment of gynaecological diseases: A review of safety and efficacy. Int J Hyperthermia [Internet]. 2015 May 3 [cited 2018 Nov 4]; 31(3):280–4. Available from: http://www.tandfonline.com/doi/full/10.3109/02656736.2014.996790 https://doi.org/10.3109/02656736.2014.996790 PMID: 25609456

6. Ikeda T, Yoshizawa S, Koizumi N, Mitsuishi M, Matsumoto Y. Focused ultrasound and lithotripsy. In: Advances in Experimental Medicine and Biology [Internet]. Springer New York LLC; 2016 [cited 2020 Sep 25]. p. 113–29. Available from: https://pubmed.ncbi.nlm.nih.gov/26486335/

7. Gallo M, Ferrara L, Naviglio D. Application of ultrasound in food science and technology: A perspective [Internet]. Vol. 7, Foods. MDPI Multidisciplinary Digital Publishing Institute; 2018 [cited 2020 Sep 25]. Available from: https://pubmed.ncbi.nlm.nih.gov/30287795/ https://doi.org/10.3390/foods7100164 PMID: 30287795

8. Chen F, Zhao ER, Hableel G, Hu T, Kim T, Li J, et al. Increasing the Efficacy of Stem Cell Therapy via Triple-Function Inorganic Nanoparticles. ACS Nano [Internet]. 2019 [cited 2020 Sep 25]; 13(6). Available from: https://pubmed.ncbi.nlm.nih.gov/31188564/ https://doi.org/10.1021/acsnano.9b00653 PMID: 31188564

9. Lemaster JE, Chen F, Kim T, Hariri A, Jokerst JV. Development of a Trimodal Contrast Agent for Acoustic and Magnetic Particle Imaging of Stem Cells. ACS Appl Nano Mater [Internet]. 2018 Mar 23 [cited 2020 Sep 25]; 1(3):1321–31. Available from: https://pubs.acs.org/doi/abs/10.1021/acsanm.8b00063

10. Heckman JD, Ryaby JP, McCabe J, Frey JJ, Kilcoyne RF. Acceleration of tibial fracture-healing by non-invasive, low-intensity pulsed ultrasound. J Bone Jt Surg—Ser A [Internet]. 1994 [cited 2020 Sep 25]; 76(1):26–34. Available from: https://pubmed.ncbi.nlm.nih.gov/8288661/ https://doi.org/10.2106/00004623-199401000-00004 PMID: 8288661

11. Kristiansen TK, Ryaby JP, McCabe J, Frey JJ, Roe LR. Accelerated healing of distal radial fractures with the use of specific, low-intensity ultrasound: A multicenter, prospective, randomized, double-blind, placebo-controlled study. J Bone Jt Surg—Ser A [Internet]. 1997 [cited 2020 Sep 25]; 79(7):961–73. Available from: https://pubmed.ncbi.nlm.nih.gov/9234872/ https://doi.org/10.2106/00004623-199707000-00002

12. Rubin C, Bolander M, Ryaby JP, Hadjiargyrou M. The use of low-intensity ultrasound to accelerate the healing of fractures [Internet]. Vol. 83, Journal of Bone and Joint Surgery—Series A. Journal of Bone and Joint Surgery Inc.; 2001 [cited 2020 Sep 25]. p. 259–70. Available from: https://pubmed.ncbi.nlm.nih.gov/11216689/ https://doi.org/10.2106/00004623-200102000-00015 PMID: 11216689

13. Zura R, Mehta S, Della Rocca GJ, Jones J, Steen RG. A cohort study of 4,190 patients treated with low-intensity pulsed ultrasound (LIPUS): Findings in the elderly versus all patients. BMC Musculoskelet Disord [Internet]. 2015 Mar 1 [cited 2020 Sep 25]; 16(1). Available from: https://pubmed.ncbi.nlm.nih.gov/25886761/ https://doi.org/10.1186/s12891-015-0498-1 PMID: 25886761

14. Tehranchi A, Badiee M, Younessian F, Badiei M, Haddadpour S. Effect of Low-intensity Pulsed Ultrasound on Postorthognathic Surgery Healing Process. Ann Maxillofac Surg [Internet]. 2017 [cited 2017 Jul 31]; 7(1):25–9. Available from: http://www.ncbi.nlm.nih.gov/pubmed/28713732 PMID: 28713732

15. Man J, Shelton RM, Cooper PR, Landini G, Scheven BA. Low intensity ultrasound stimulates osteoblast migration at different frequencies. J Bone Miner Metab [Internet]. 2012 Sep [cited 2020 Sep 25]; 30 (5):602–7. Available from: https://pubmed.ncbi.nlm.nih.gov/22752127/ https://doi.org/10.1007/s00774-012-0368-y PMID: 22752127

16. Yilmaz V, Karadas O, Dandinoglu T, Umay E, Cakci A, Tan AK. Efficacy of extracorporeal shockwave therapy and lowintensity pulsed ultrasound in a rat knee osteoarthritis model: A randomized controlled trial. Eur J Rheumatol [Internet]. 2017 Jun 12 [cited 2020 Sep 25]; 4(2):104–8. Available from: https://pubmed.ncbi.nlm.nih.gov/28638681/ https://doi.org/10.5152/eurjrheum.2017.160089 PMID: 28638681

17. Atherton P, Lausecker F, Harrison A, Ballestrem C. Low-intensity pulsed ultrasound promotes cell motility through vinculin-controlled Rac1 GTPase activity. J Cell Sci [Internet]. 2017 Jul 15 [cited 2018 Jun 3]; 130(14):2277–91. Available from: http://www.ncbi.nlm.nih.gov/pubmed/28576970 https://doi.org/10.1242/jcs.192781 PMID: 28576970

18. Bernal A, Pérez LM, De Lucas B, Martín NS, Kadow-Romacker A, Plaza G, et al. Low-Intensity Pulsed Ultrasound Improves the Functional Properties of Cardiac Mesoangioblasts. Stem Cell Rev Reports. 2015; 11(6). https://doi.org/10.1007/s12015-015-9608-6 PMID: 26201830

19. Kösters AK, Ganse B, Gueorguiev B, Klos K, Modabber A, Nebelung S, et al. Effects of low-intensity pulsed ultrasound on soft tissue micro-circulation in the foot. Int Orthop [Internet]. 2017 Jul 22 [cited 2017 Jul 31];1–8. Available from: http://link.springer.com/10.1007/s00264-017-3574-3

20. Lu Z-Y, Li R-L, Zhou H-S, Huang J-J, Su Z-X, Qi J, et al. Therapeutic ultrasound reverses peripheral ischemia in type 2 diabetic mice through PI3K-Akt-eNOS pathway. Am J Transl Res [Internet]. 2016 [cited 2020 Sep 25]; 8(9):3666–77. Available from: http://www.ncbi.nlm.nih.gov/pubmed/27725849 PMID: 27725849

21. Padilla F, Puts R, Vico L, Raum K. Stimulation of bone repair with ultrasound: A review of the possible mechanic effects. Ultrasonics [Internet]. 2014 Jul [cited 2017 Jul 31]; 54(5):1125–45. Available from: http://linkinghub.elsevier.com/retrieve/pii/S0041624X14000055 https://doi.org/10.1016/j.ultras.2014.01.004 PMID: 24507669

22. Warden SJ, Fuchs RK, Kessler CK, Avin KG, Cardinal RE, Stewart RL. Ultrasound produced by a conventional therapeutic ultrasound unit accelerates fracture repair. Phys Ther [Internet]. 2006 Aug [cited 2018 Jun 3]; 86(8):1118–27. Available from: http://www.ncbi.nlm.nih.gov/pubmed/16879045 PMID: 16879045

23. Chen Y, Xiang L-X, Shao J-Z, Pan R-L, Wang Y-X, Dong X-J, et al. Recruitment of endogenous bone marrow mesenchymal stem cells towards injured liver. J Cell Mol Med [Internet]. 2010 Jun [cited 2017 Apr 16]; 14(6B):1494–508. Available from: http://www.ncbi.nlm.nih.gov/pubmed/19780871 https://doi.org/10.1111/j.1582-4934.2009.00912.x PMID: 19780871

24. da Silva Meirelles L, Chagastelles PC, Nardi NB. Mesenchymal stem cells reside in virtually all postnatal organs and tissues. J Cell Sci [Internet]. 2006 May 9 [cited 2018 May 23]; 119(11):2204–13. Available from: http://www.ncbi.nlm.nih.gov/pubmed/16684817 https://doi.org/10.1242/jcs.02932 PMID: 16684817

25. Robey P. "Mesenchymal stem cells": Fact or fiction, and implications in their therapeutic use [Internet]. Vol. 6, F1000Research. Faculty of 1000 Ltd; 2017 [cited 2020 Sep 25]. Available from: https://pubmed.ncbi.nlm.nih.gov/28491279/ https://doi.org/10.12688/f1000research.10955.1 PMID: 28491279

26. Bernal A, San Martin N, Fernandez M, Covarello D, Molla F, Soldo A, et al. L-selectin and SDF-1 enhance the migration of mouse and human cardiac mesoangioblasts. Cell Death Differ [Internet]. 2012; 19(2):345–55. Available from: http://www.ncbi.nlm.nih.gov/pubmed/21869829 https://doi.org/10.1038/cdd.2011.110 PMID: 21869829

27. Roper JA, Williamson RC, Bally B, Cowell CAM, Brooks R, Stephens P, et al. Ultrasonic Stimulation of Mouse Skin Reverses the Healing Delays in Diabetes and Aging by Activation of Rac1. J Invest Dermatol [Internet]. 2015 Nov [cited 2018 May 26]; 135(11):2842–51. Available from: http://www.ncbi.nlm.nih.gov/pubmed/26079528 https://doi.org/10.1038/jid.2015.224 PMID: 26079528

28. Zhang L, Zhang W, Orsi F, Chen W, Wang Z. Ultrasound-guided high intensity focused ultrasound for the treatment of gynaecological diseases: A review of safety and efficacy. Int J Hyperth [Internet]. 2015 Apr 3 [cited 2020 Sep 25]; 31(3):280–4. Available from: http://www.tandfonline.com/doi/full/10.3109/02656736.2014.996790

29. Bohari SP, Grover LM, Hukins DW. Pulsed low-intensity ultrasound increases proliferation and extracelluar matrix production by human dermal fibroblasts in three-dimensional culture. J Tissue Eng [Internet]. 2015 [cited 2017 Mar 12]; 6:2041731415615777. Available from: http://www.ncbi.nlm.nih.gov/pubmed/26668710 https://doi.org/10.1177/2041731415615777 PMID: 26668710

30. De Ávila Santana L, Alves JM, Andrade TAM, Kajiwara JK, Garcia SB, Gomes FG, et al. Clinical and immunohistopathological aspects of venous ulcers treatment by Low-Intensity Pulsed Ultrasound (LIPUS). Ultrasonics [Internet]. 2013 Apr [cited 2020 Sep 25]; 53(4):870–9. Available from: https://pubmed.ncbi.nlm.nih.gov/23294989/ https://doi.org/10.1016/j.ultras.2012.12.009 PMID: 23294989

31. Bernal A, Fernandez M, Perez LM, San Martin N, Galvez BG. Method for obtaining committed adult mesenchymal precursors from skin and lung tissue. PLoS One [Internet]. 2012; 7(12):e53215. Available from: http://www.ncbi.nlm.nih.gov/pubmed/23300894 https://doi.org/10.1371/journal.pone.0053215 PMID: 23300894

32. Leskinen JJ, Hynynen K. Study of Factors Affecting the Magnitude and Nature of Ultrasound Exposure with In Vitro Set-Ups. Ultrasound Med Biol [Internet]. 2012 May [cited 2020 Sep 25]; 38(5):777–94. Available from: https://pubmed.ncbi.nlm.nih.gov/22425382/ https://doi.org/10.1016/j.ultrasmedbio.2012.01.019 PMID: 22425382

33. Robinson MD, McCarthy DJ, Smyth GK. edgeR: A Bioconductor package for differential expression analysis of digital gene expression data. Bioinformatics [Internet]. 2009 Nov 11 [cited 2020 Sep 25]; 26 (1):139–40. Available from: https://pubmed.ncbi.nlm.nih.gov/19910308/ https://doi.org/10.1093/bioinformatics/btp616 PMID: 19910308

34. Zhou S, Schmelz A, Seufferlein T, Li Y, Zhao J, Bachem MG. Molecular Mechanisms of Low Intensity Pulsed Ultrasound in Human Skin Fibroblasts. J Biol Chem [Internet]. 2004 Dec 24 [cited 2018 May 31]; 279(52):54463–9. Available from: http://www.ncbi.nlm.nih.gov/pubmed/15485877 https://doi.org/10.1074/jbc.M404786200 PMID: 15485877

35. Tsai W-C, Pang J-HS, Hsu C-C, Chu N-K, Lin M-S, Hu C-F. Ultrasound stimulation of types I and III collagen expression of tendon cell and upregulation of transforming growth factor β. J Orthop Res [Internet]. 2006 Jun [cited 2018 May 31]; 24(6):1310–6. Available from: http://www.ncbi.nlm.nih.gov/pubmed/16705693 https://doi.org/10.1002/jor.20130 PMID: 16705693

36. Boyle ST, Samuel MS. Mechano-reciprocity is maintained between physiological boundaries by tuning signal flux through the Rho-associated protein kinase [Internet]. Vol. 7, Small GTPases. Taylor and Francis Inc.; 2016 [cited 2020 Dec 9]. p. 139–46. Available from: /pmc/articles/PMC5003540/?report=abstract https://doi.org/10.1080/21541248.2016.1173771 PMID: 27168253

37. Dupont S, Morsut L, Aragona M, Enzo E, Giulitti S, Cordenonsi M, et al. Role of YAP/TAZ in mechanotransduction. Nature [Internet]. 2011 Jun 8 [cited 2020 Dec 9]; 474(7350):179–84. Available from: https://pubmed.ncbi.nlm.nih.gov/21654799/ https://doi.org/10.1038/nature10137 PMID: 21654799

38. Nagao M, Tanabe N, Manaka S, Naito M, Sekino J, Takayama T, et al. LIPUS suppressed LPS-induced IL-1α through the inhibition of NF-κB nuclear translocation via AT1-PLCβ pathway in MC3T3-E1 cells. J Cell Physiol [Internet]. 2017 Dec 1 [cited 2020 Sep 25]; 232(12):3337–46. Available from: https://pubmed.ncbi.nlm.nih.gov/28063227/ https://doi.org/10.1002/jcp.25777 PMID: 28063227

39. Lv Y, Zhao P, Chen G, Sha Y, Yang L. Effects of low-intensity pulsed ultrasound on cell viability, proliferation and neural differentiation of induced pluripotent stem cells-derived neural crest stem cells. Biotechnol Lett [Internet]. 2013 Dec [cited 2020 Sep 25]; 35(12):2201–12. Available from: https://pubmed.ncbi.nlm.nih.gov/24078117/ https://doi.org/10.1007/s10529-013-1313-4 PMID: 24078117

40. Chan CW, Qin L, Lee KM, Cheung WH, Cheng JCY, Leung KS. Dose-dependent effect of low-intensity pulsed ultrasound on callus formation during rapid distraction osteogenesis. J Orthop Res [Internet]. 2006 Nov [cited 2020 Sep 25]; 24(11):2072–9. Available from: https://pubmed.ncbi.nlm.nih.gov/16917923/ https://doi.org/10.1002/jor.20258 PMID: 16917923

41. Zhao L, Feng Y, Shi A, Zhang L, Guo S, Wan M. Neuroprotective Effect of Low-Intensity Pulsed Ultrasound Against MPP+-Induced Neurotoxicity in PC12 Cells: Involvement of K2P Channels and Stretch-Activated Ion Channels. Ultrasound Med Biol [Internet]. 2017 Sep 1 [cited 2020 Sep 25]; 43(9):1986–99. Available from: https://pubmed.ncbi.nlm.nih.gov/28583325/ https://doi.org/10.1016/j.ultrasmedbio.2017.04.020 PMID: 28583325

42. Zura R, Xu Z, Della Rocca GJ, Mehta S, Steen RG. When Is a Fracture Not "fresh"? Aligning Reimbursement with Patient Outcome after Treatment with Low-Intensity Pulsed Ultrasound. In: Journal of Orthopaedic Trauma [Internet]. Lippincott Williams and Wilkins; 2017 [cited 2020 Sep 25]. p. 248–51. Available from: https://pubmed.ncbi.nlm.nih.gov/28134628/ https://doi.org/10.1097/BOT.0000000000000778 PMID: 28134628

43. Huang JJ, Shi YQ, Li RL, Hu A, Lu ZY, Weng L, et al. Angiogenesis effect of therapeutic ultrasound on HUVECs through activation of the PI3K-Akt-eNOS signal pathway. Am J Transl Res [Internet]. 2015 Feb 25 [cited 2020 Sep 25]; 7(6):1106–15. Available from: www.ajtr.org PMID: 26279754

44. Iwanabe Y, Masaki C, Tamura A, Tsuka S, Mukaibo T, Kondo Y, et al. The effect of low-intensity pulsed ultrasound on wound healing using scratch assay in epithelial cells. J Prosthodont Res [Internet]. 2016 Oct [cited 2017 Jul 25]; 60(4):308–14. Available from: http://linkinghub.elsevier.com/retrieve/pii/S1883195816300019 https://doi.org/10.1016/j.jpor.2016.03.002 PMID: 27026212

45. Feril LB, Kondo T, Cui ZG, Tabuchi Y, Zhao QL, Ando H, et al. Apoptosis induced by the sonomechanical effects of low intensity pulsed ultrasound in a human leukemia cell line. Cancer Lett [Internet]. 2005 Apr 28 [cited 2020 Nov 19]; 221(2):145–52. Available from: https://pubmed.ncbi.nlm.nih.gov/15808400/ https://doi.org/10.1016/j.canlet.2004.08.034 PMID: 15808400

46. Shi M, Liu B, Liu G, Wang P, Yang M, Li Y, et al. Low intensity-pulsed ultrasound induced apoptosis of human hepatocellular carcinoma cells in vitro. Ultrasonics [Internet]. 2016 Jan 1 [cited 2020 Nov 19]; 64:43–53. Available from: https://pubmed.ncbi.nlm.nih.gov/26231998/ https://doi.org/10.1016/j.ultras.2015.07.011 PMID: 26231998

47. Lagneaux L, De Meulenaer EC, Delforge A, Dejeneffe M, Massy M, Moerman C, et al. Ultrasonic low-energy treatment: A novel approach to induce apoptosis in human leukemic cells. Exp Hematol [Internet]. 2002 Nov 1 [cited 2021 Jan 12]; 30(11):1293–301. Available from: https://pubmed.ncbi.nlm.nih.gov/12423682/ https://doi.org/10.1016/s0301-472x(02)00920-7 PMID: 12423682

48. Qiu Z, Guo J, Kala S, Zhu J, Xian Q, Qiu W, et al. The Mechanosensitive Ion Channel Piezo1 Significantly Mediates In Vitro Ultrasonic Stimulation of Neurons. iScience [Internet]. 2019 Nov 22 [cited 2020 Nov 19]; 21:448–57. Available from: /pmc/articles/PMC6849147/?report=abstract https://doi.org/10.1016/j.isci.2019.10.037 PMID: 31707258

49. Prieto ML, Firouzi K, Khuri-Yakub BT, Maduke M. Activation of Piezo1 but Not NaV1.2 Channels by Ultrasound at 43 MHz. Ultrasound Med Biol [Internet]. 2018 Jun 1 [cited 2020 Nov 19]; 44(6):1217–32. Available from: https://pubmed.ncbi.nlm.nih.gov/29525457/ https://doi.org/10.1016/j.ultrasmedbio.2017.12.020 PMID: 29525457

50. Gao Q, Cooper PR, Walmsley AD, Scheven BA. Role of Piezo Channels in Ultrasound-stimulated Dental Stem Cells. J Endod [Internet]. 2017 Jul 1 [cited 2020 Nov 19]; 43(7):1130–6. Available from: https://pubmed.ncbi.nlm.nih.gov/28527849/ https://doi.org/10.1016/j.joen.2017.02.022 PMID: 28527849

51. Paluch EK, Nelson CM, Biais N, Fabry B, Moeller J, Pruitt BL, et al. Mechanotransduction: Use the force(s). BMC Biol [Internet]. 2015 Jul 4 [cited 2020 Sep 25]; 13(1). Available from: https://pubmed.ncbi.nlm.nih.gov/26141078/

52. Samandari M, Abrinia K, Mokhtari-Dizaji M, Tamayol A. Ultrasound induced strain cytoskeleton rearrangement: An experimental and simulation study. J Biomech [Internet]. 2017 Jul 26 [cited 2018 May 27]; 60:39–47. Available from: http://www.ncbi.nlm.nih.gov/pubmed/28757237 https://doi.org/10.1016/j.jbiomech.2017.06.003 PMID: 28757237

53. Zhou S, Schmelz A, Seufferlein T, Li Y, Zhao J, Bachem MG. Molecular mechanisms of low intensity pulsed ultrasound in human skin fibroblasts. J Biol Chem [Internet]. 2004 Dec 24 [cited 2020 Sep 25]; 279(52):54463–9. Available from: https://pubmed.ncbi.nlm.nih.gov/15485877/ https://doi.org/10.1074/jbc.M404786200 PMID: 15485877

54. Hebert MD. Signals controlling Cajal body assembly and function [Internet]. Vol. 45, International Journal of Biochemistry and Cell Biology. Elsevier Ltd; 2013 [cited 2020 Sep 25]. p. 1314–7. Available from: https://pubmed.ncbi.nlm.nih.gov/23583661/ https://doi.org/10.1016/j.biocel.2013.03.019 PMID: 23583661

55. Karijolich J, Yu YT. Spliceosomal snRNA modifications and their function [Internet]. Vol. 7, RNA Biology. Taylor and Francis Inc.; 2010 [cited 2020 Sep 25]. p. 192–204. Available from: https://pubmed.ncbi.nlm.nih.gov/20215871/ https://doi.org/10.4161/rna.7.2.11207 PMID: 20215871

56. Lafarga M, Tapia O, Romero AM, Berciano MT. Cajal bodies in neurons [Internet]. Vol. 14, RNA Biology. Taylor and Francis Inc.; 2017 [cited 2020 Sep 25]. p. 712–25. Available from: https://pubmed.ncbi.nlm.nih.gov/27627892/ https://doi.org/10.1080/15476286.2016.1231360 PMID: 27627892

57. Poh YC, Shevtsov SP, Chowdhury F, Wu DC, Na S, Dundr M, et al. Dynamic force-induced direct dissociation of protein complexes in a nuclear body in living cells. Nat Commun [Internet]. 2012 [cited 2020 Sep 25]; 3. Available from: https://pubmed.ncbi.nlm.nih.gov/22643893/

58. Wang N, Tytell JD, Ingber DE. Mechanotransduction at a distance: Mechanically coupling the extracellular matrix with the nucleus [Internet]. Vol. 10, Nature Reviews Molecular Cell Biology. Nat Rev Mol Cell Biol; 2009 [cited 2020 Sep 25]. p. 75–82. Available from: https://pubmed.ncbi.nlm.nih.gov/19197334/

59. Carovac A, Smajlovic F, Junuzovic D. Application of Ultrasound in Medicine. Acta Inform Medica [Internet]. 2011 [cited 2020 Sep 25]; 19(3):168. Available from: /pmc/articles/PMC3564184/?report=abstract PMID: 23408755

60. Monden K, Sasaki H, Yoshinari M, Yajima Y. Effect of low-intensity pulsed ultrasound (LIPUS) with different frequency on bone defect healing. J Hard Tissue Biol. 2015 Apr 14; 24(2):189–98.

61. Zhao X, Zhao G, Shi Z, Zhou C, Chen Y, Hu B, et al. Low-intensity pulsed ultrasound (LIPUS) prevents periprosthetic inflammatory loosening through FBXL2-TRAF6 ubiquitination pathway. Sci Rep [Internet]. 2017 Apr 5 [cited 2020 Sep 25]; 7(1):1–11. Available from: www.nature.com/scientificreports/

62. Fung CH, Cheung WH, Pounder NM, de Ana FJ, Harrison A, Leung KS. Effects of Different Therapeutic Ultrasound Intensities on Fracture Healing in Rats. Ultrasound Med Biol [Internet]. 2012 [cited 2020 Sep 25]; 38(5):745–52. Available from: https://pubmed.ncbi.nlm.nih.gov/22425380/ https://doi.org/10.1016/j.ultrasmedbio.2012.01.022 PMID: 22425380

63. Saito M, Soshi S, Tanaka T, Fujii K. Intensity-related differences in collagen post-translational modification in MC3T3-E1 osteoblasts after exposure to low- and high-intensity pulsed ultrasound. Bone [Internet]. 2004 Sep [cited 2020 Sep 25]; 35(3):644–55. Available from: https://pubmed.ncbi.nlm.nih.gov/15336600/ https://doi.org/10.1016/j.bone.2004.04.024 PMID: 15336600

64. Angle SR, Sena K, Sumner DR, Virdi AS. Osteogenic differentiation of rat bone marrow stromal cells by various intensities of low-intensity pulsed ultrasound. Ultrasonics [Internet]. 2011 Apr [cited 2020 Sep 25]; 51(3):281–8. Available from: https://pubmed.ncbi.nlm.nih.gov/20965537/ https://doi.org/10.1016/j.ultras.2010.09.004 PMID: 20965537